Kinetics and Catalysis, Vol. 44, No. 4, 2003, pp. 575–582. Translated from Kinetika i Kataliz, Vol. 44, No. 4, 2003, pp. 629–637.

CATALYTIC
REACTION MECHANISMS

Comparative XPS Study of Al_2O_3 and CeO_2 Sulfation in Reactions with SO_2, $SO_2 + O_2$, $SO_2 + H_2O$, and $SO_2 + O_2 + H_2O$

M. Yu. Smirnov*, A. V. Kalinkin*, A. V. Pashis*, A. M. Sorokin*,
A. S. Noskov*, V. I. Bukhtiyarov*, K. C. Kharas, and M. A. Rodkin****
** Boreskov Institute of Catalysis, Siberian Division, Russian Academy of Sciences, Novosibirsk, 630090 Russia*
*** Delphi Automotive Systems, Tulsa, OK 74158-0970, USA*
Received October 9, 2002

Abstract—The interactions of Al_2O_3, CeO_2, Pt/Al_2O_3, and Pt/CeO_2 films with SO_2, $SO_2 + H_2O$, $SO_2 + O_2$, and $SO_2 + O_2 + H_2O$ in the temperature range 300–673 K at the partial pressures of SO_2, O_2, and H_2O equal to 1.5×10^2, 1.5×10^2, and 3×10^2 Pa, respectively, were studied using X-ray photoelectron spectroscopy. The formation of surface sulfite at $T \geq 473$ K (the S $2p_{3/2}$ binding energy (E_b) is 167.5 eV) and surface sulfate at $T \geq 573$ K (E_b = 169.2 eV) was observed in the reactions of Al_2O_3 and CeO_2 with SO_2. The formation of sulfates on the surface of CeO_2 occurred much more effectively than in the case of Al_2O_3, and it was accompanied by the reduction of Ce(IV) to Ce(III). The formation of aluminum and cerium sulfates and sulfites on model Pt/Al_2O_3 and Pt/CeO_2 catalysts occurred simultaneously with the formation of surface platinum sulfides (E_b of S $2p_{3/2}$ is 162.2 eV). The effects of oxygen and water vapor on the nature and yield of sulfur-containing products were studied.

INTRODUCTION

The surface sulfation of oxide catalyst components (Al_2O_3, CeO_2, etc.) is one of the factors responsible for a decrease in the activity of automotive pollution control catalysts upon reaction with SO_2, which is formed as an impurity in fuel combustion [1]. This fact explains the great number of publications devoted to the reactions of SO_2 with the oxides Al_2O_3 [2–12] and CeO_2 [7, 9, 13–15] and with the model catalysts Pt/Al_2O_3 [16, 17] and Pt/CeO_2 [18, 19]. However, studies performed under different conditions with the use of different techniques gave contradictory results. Moreover, as a rule, the attention of researchers has been focused on the nature of sulfur-containing products. Attempts to characterize the effect of SO_2 on the state of a metal as the constituent of an oxide and a metal supported on the oxide were made in only a very few publications. According to IR-spectroscopic data, the reactions of SO_2 with Al_2O_3, CeO_2, Pt/Al_2O_3, and Pt/CeO_2 at near-atmospheric pressures over a wide temperature range resulted in the formation of sulfites [2–9, 13, 19], whereas aluminum sulfate [2, 3, 6, 8, 11, 12, 16] or cerium sulfate [13, 18, 19] were obtained in a mixture of $SO_2 + O_2$ at elevated temperatures (≥673 K). Sulfate formation on the surface of CeO_2 was accompanied by cerium reduction to Ce^{3+} [18, 19]. At the same time, according to data obtained by X-ray photoelectron spectroscopy (XPS), the reactions of Al_2O_3 and CeO_2 with SO_2 even at $T \sim 100$–353 K and small exposures to the gas can result in not only sulfites [15, 20] but also sulfates even in the absence of oxygen [14, 20]. In this case, in contrast to results obtained at elevated temperatures and pressures, the formation of sulfates on CeO_2 occurred without changes in the oxidation state of cerium; on this basis, it was assumed that SO_2 underwent disproportionation to $Ce(SO_4)_2$ and SO [14].

In this work, we attempted to find which reactions occur during the interaction of SO_2 and $SO_2 + O_2$ with the oxides Al_2O_3 and CeO_2 and the model catalysts Pt/Al_2O_3 and Pt/CeO_2 depending on temperature. For this purpose, we performed an XPS study on both the nature of sulfur-containing products and the oxidation states of the metal constituents of the oxides and metals supported on oxide surfaces. We also studied the reactions of the above systems with $SO_2 + H_2O$ and $SO_2 + O_2 + H_2O$ mixtures in order to detect the effect of water vapor. Considerable amounts of water vapor occur in gases to be purified, including automotive exhausts; however, water vapor has received undeservedly little attention in the studies of model systems.

EXPERIMENTAL

The XPS study was performed on a VG ESCA-3 instrument. The Al K_α line with $h\nu$ = 1486.6 eV was used as exciting radiation. The constant resolution mode with the analyzer pass energy HV = 20 eV was used to record the XPS spectra. The positions of XPS lines (taking into account the charging effect) were determined with reference to the Al2*p* line in the case

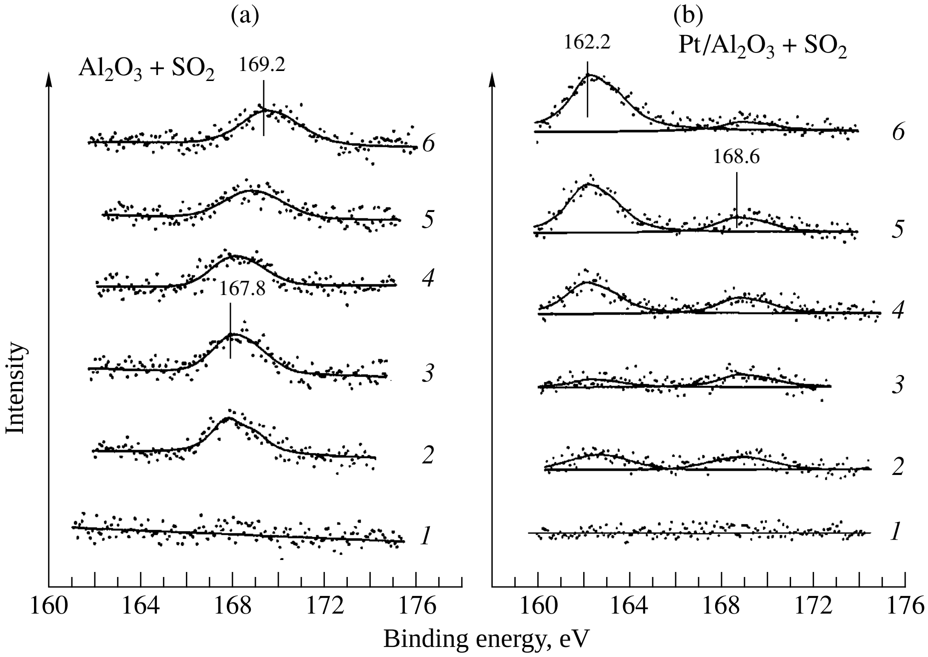

Fig. 1. XPS S2*p* spectra of (a) Al_2O_3 and (b) Pt/Al_2O_3 (*1*) before and after the reaction with SO_2 at $P_{SO_2} = 1.5 \times 10^2$ Pa and *T*, K: (*2*) 300, (*3*) 373, (*4*) 473, (*5*) 573, and (*6*) 673.

of Al_2O_3 (E_b = 74.5 eV) or the *u*''' satellite line in the Ce3*d* spectrum in the case of CeO_2 (E_b = 916.7 eV) [21].

The ceria and alumina samples were prepared in the preparation chamber of the spectrometer in the form of thin films on a tantalum foil substrate. The design of the holder allowed us to heat the samples by passing current through the tantalum foil. The temperature was monitored with a Chromel–Alumel thermocouple welded to the underside of the foil.

A film of alumina on the surface of tantalum foil was obtained by the sputtering of aluminum in oxygen at the pressure $P_{O_2} \approx 5 \times 10^{-3}$ Pa onto the foil followed by treatment in O_2 at 1.5×10^{-2} Pa and 873 K. A film of CeO_2 was obtained by the sputtering of cerium metal onto the preformed film of Al_2O_3 (barrier layer) with the subsequent oxidation of cerium in oxygen at $P_{O_2} \approx 1.5 \times 10^{-3}$ Pa and $T \approx 873$ K. Only lines intrinsic to Al and O or Ce and O were detected in the XPS spectra of the films prepared. Platinum was sputtered onto the surface of precleaned oxide films. Previously, a similar procedure was used for preparing oxide films and the samples of Rh/TiO_2 [22] and Pd/Fe_2O_3 [23] model catalysts.

The reactions were performed in the preparation chamber of the electron spectrometer. The oxide films were treated at the partial pressures of SO_2, O_2, and H_2O equal to 1.5×10^2, 1.5×10^2, and 3×10^2 Pa, respectively, over the temperature range 300–673 K for 20 min. After pumping out the reaction mixture to a background pressure ($<10^{-6}$ Pa), the sample was placed in the analyzer chamber for measuring the XPS spectra. Before experiments with a new reaction mixture, the sample was annealed in oxygen at $P_{O_2} \approx 1.5 \times 10^{-2}$ Pa and $T \approx 873$ K until the complete removal of sulfur-containing particles. This procedure also removed carbon, which was formed in the course of the adsorption of background hydrocarbons, from platinum.

RESULTS

Al_2O_3 and Pt/Al_2O_3

Figure 1 demonstrates the XPS S2*p* spectra measured after the reactions of the films of alumina and alumina with sputtered platinum with SO_2 at specified temperatures. The asymmetry of the detected signals is due to the occurrence of two components in each of them. These $S2p_{3/2}$ and $S2p_{1/2}$ components result from spin–orbital splitting, which is equal to 1.2 eV for S2*p* lines. The binding energy was determined for the more intense $S2p_{3/2}$ component after the deconvolution of the resulting line.

The spectra presented in Fig. 1a suggest that sulfur-containing products were formed upon the interaction of Al_2O_3 with SO_2 at $T \leq 473$ K. These products are characterized by the $S2p_{3/2}$ line with $E_b \approx 167.8$ eV, which is typical of sulfites [24]. As the reaction temperature was increased, the line was shifted to greater binding energies, so that after treatment at 673 K the E_b of $S2p_{3/2}$ became equal to 169.2 eV, which is character-

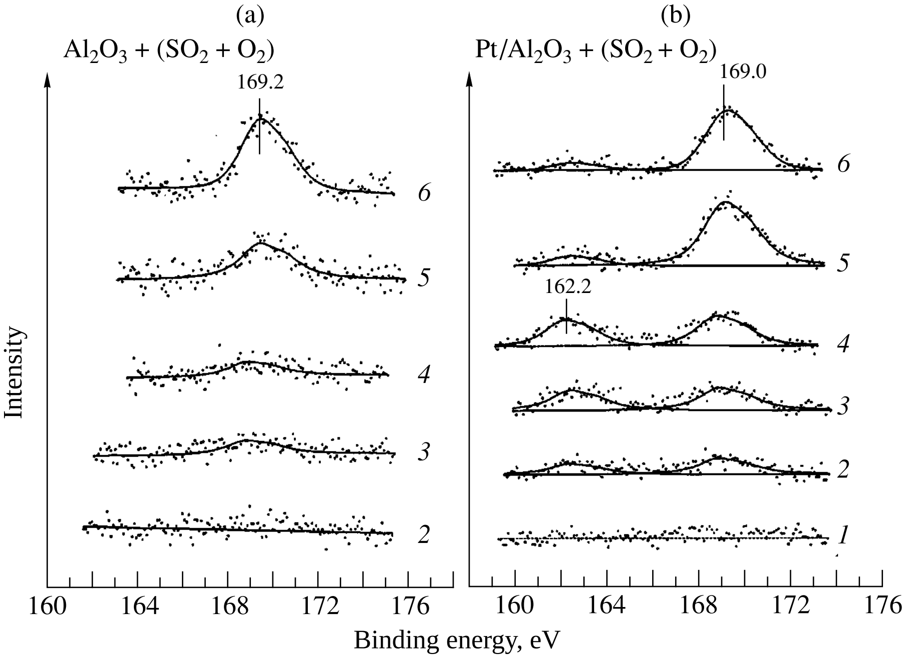

Fig. 2. XPS S2*p* spectra of (a) Al_2O_3 and (b) Pt/Al_2O_3 (*1*) before and after the reaction with a mixture of SO_2 and O_2 at $P_{SO_2} = P_{O_2} = 1.5 \times 10^2$ Pa and *T*, K: (*2*) 300, (*3*) 373, (*4*) 473, (*5*) 573, and (*6*) 673.

istic of sulfates [24]. The series of spectra in the S2*p* region measured after the interaction of Al_2O_3 with a mixture of SO_2 and H_2O (not shown in Fig. 1) suggests the formation of the above products: sulfites at $T \leq 473$ K and sulfates at higher temperatures. However, the yield of products was much lower than that in the case of reactions with pure SO_2.

The interaction of SO_2 with Pt/Al_2O_3 is characterized by the simultaneous appearance of two lines in the XPS spectrum (Fig. 1b). In addition to a line observed in the $S2p_{3/2}$ binding energy region 168.5–168.8 eV, which can be attributed to a sulfite and sulfate mixture formed on the surface of alumina, a second more intense line with a binding energy of 162.2 eV appeared. This low value of E_b indicates that sulfur is not bound to the oxygen atom in the corresponding surface compound; that is, it can be the constituent of platinum sulfide or elemental sulfur adsorbed on the surface of Pt. The S2*p* line of metal sulfides is found in the region ~160–163.5 eV [24], in particular, at 163.6 eV for the platinum sulfide PtS [25]. Elemental sulfur is characterized by the binding energy of S2*p* in the region 164.0–164.8 eV [24]. Sulfur and platinum sulfide, which were formed as a result of H_2S decomposition on the surface of a Pt/SiO_2 catalyst, were characterized by the S2*p* lines with binding energies of ~164.0 and ~162.5 eV, respectively [26]. Based on the value $E_b(S2p_{3/2}) = 162.2$ eV (Fig. 1b), it is likely that, in our case, this signal should be preferably attributed to sulfide ions on the surface of platinum rather than in the structure of bulk compounds. This conclusion is consistent with the constancy of the binding energy of the $Pt4f_{7/2}$ line (~71.1–71.3 eV), which is characteristic of platinum metal in the interaction of Pt/Al_2O_3 with SO_2.

Figure 2 demonstrates a series of the S2*p* spectra recorded after the interaction of Al_2O_3 and Pt/Al_2O_3 with $SO_2 + O_2$. It can be seen that the addition of O_2 to SO_2 inhibited the formation of sulfites at moderate temperatures (Fig. 2a). Sulfate, whose yield increased with temperature, was the predominant product on the surface of aluminum oxide at temperatures of ≥373 K. On the addition of water vapor to a mixture of SO_2 and O_2 (as in the case of SO_2/Al_2O_3, the spectra are not shown), the tendency of alumina toward sulfation was significantly suppressed. When Pt/Al_2O_3 reacted with a mixture of SO_2 and oxygen (Fig. 2b), the formation of two types of products was observed: aluminum sulfate and sulfide ions on the surface of platinum, which are characterized by the $S2p_{3/2}$ lines with binding energies of 169.0 and 162.2 eV, respectively. In the reaction with pure SO_2, sulfide was the main product over the entire range of temperatures, whereas sulfide and sulfate were formed in approximately equal amounts in the presence of oxygen at $T \leq 473$ K. Sulfate became the predominant product at higher temperatures. The yield of surface platinum sulfide dramatically decreased at $T > 473$ K.

A quantitative comparison of the intensities of the S2*p* lines of sulfates after normalization to the intensities of the corresponding Al2*p* lines measured at the same reaction temperatures suggests that the sulfating

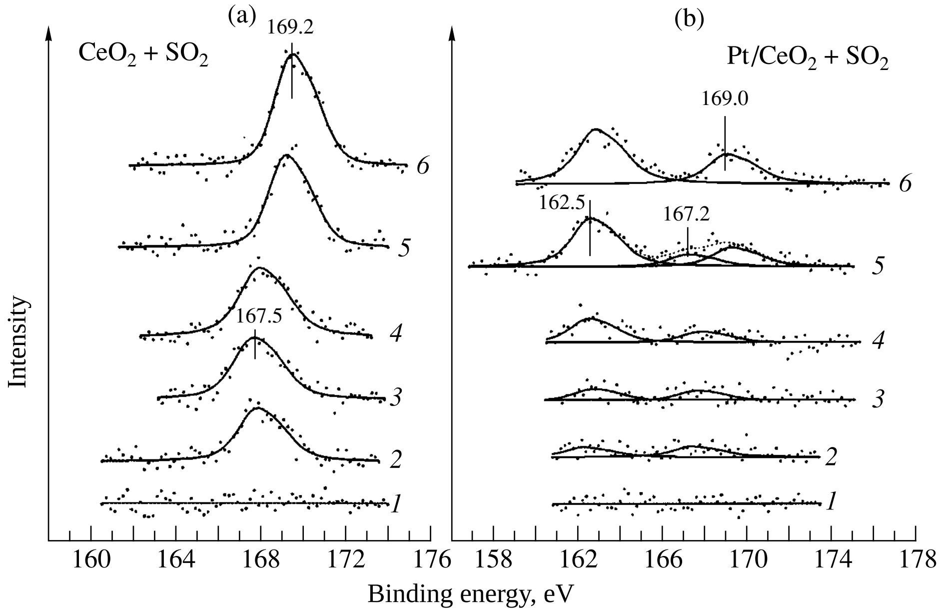

Fig. 3. XPS S2*p* spectra of (a) CeO_2 and (b) Pt/CeO_2 (*1*) before and after the reaction with SO_2 at $P_{SO_2} = 1.5 \times 10^2$ Pa and *T*, K: (*2*) 300, (*3*) 373, (*4*) 473, (*5*) 573, and (*6*) 673.

ability of various SO_2-containing atmospheres with respect to alumina decreased in the following order:

$$Al_2O_3\text{: } (SO_2 + O_2) > SO_2 \\ > (SO_2 + O_2 + H_2O) > (SO_2 + H_2O). \quad (1)$$

Thus, the presence of oxygen facilitates and the presence of water vapor hinders sulfate formation on Al_2O_3.

CeO_2 and Pt/CeO_2

Figure 3 demonstrates the S2*p* spectra measured after the interaction of CeO_2 and Pt/CeO_2 with SO_2. The series of spectra in Fig. 3a indicates that the interaction of CeO_2 with SO_2 gave products that were qualitatively similar to those observed in the case of Al_2O_3: sulfites at $T \leq 473$ K and sulfates at $T > 473$ K, as indicated by the appearance of S2*p* lines with $E_b(S2p_{3/2})$ ~167.5–167.8 and 169.2 eV, respectively. The addition of H_2O to SO_2 did not affect the chemical nature of the resulting products; however, the yield of products noticeably decreased as compared with the reaction with pure SO_2.

As in the case of Pt/Al_2O_3, two types of products were observed in the reaction of SO_2 with Pt/CeO_2 over the entire range of temperatures (Fig. 3b). Platinum sulfide (E_b of $S2p_{3/2}$ is 162.5 eV) was one of the products. The temperature dependence of E_b and the intensity of the second peak is identical to that observed for cerium dioxide without sputtered platinum. Consequently, we can state that, in this case, the formation of sulfite at $T \leq$ 473 K and sulfate at $T \geq 573$ K also took place on the surface of CeO_2. A comparison with the behavior of Pt/Al_2O_3 indicates that cerium dioxide as the constituent of Pt/CeO_2 is more prone to sulfation than alumina in Pt/Al_2O_3.

The series of the S2*p* spectra in Fig. 4a, which were measured after the reaction of CeO_2 with a mixture of SO_2 and O_2 at the specified temperatures, indicates that, starting with a temperature of 473 K, sulfate was the predominant product, as in the case with Al_2O_3. The addition of water to a mixture of SO_2 and oxygen significantly increased the yield of sulfate; this is the difference between the behaviors of CeO_2 and Al_2O_3 (the spectra are not shown). The interaction of Pt/CeO_2 with a mixture of SO_2 and oxygen mainly resulted in the formation of sulfate, whose yield increased with reaction temperature (Fig. 4b). Sulfide was detected in considerable amounts only after the reaction at 373 K.

Another difference, which is most significant, between systems based on CeO_2 and aluminum oxide systems consists in a change in the chemical state of cerium under the action of SO_2-containing mixtures. The state of aluminum in Al_2O_3 and Pt/Al_2O_3 remained unchanged, whereas cerium reduction was observed in the films of CeO_2 and Pt/CeO_2. This conclusion follows from the Ce3*d* spectra presented in Fig. 5. These spectra were measured after the reactions of SO_2 and a mixture of $SO_2 + O_2$ with CeO_2 and Pt/CeO_2 at 673 K. At the bottom of Fig. 5, the spectra of the initial samples of pure CeO_2 and Pt/CeO_2 surfaces before the interaction with SO_2-containing mixtures are shown. The background lines and the results of the deconvolution of spectral contours are also shown for all the spectra in Fig. 5. The initial spectra of both samples contained three lines in each component of the $Ce3d_{5/2}$–$Ce3d_{3/2}$ doublet, which characterize the Ce(IV) state. It is com-

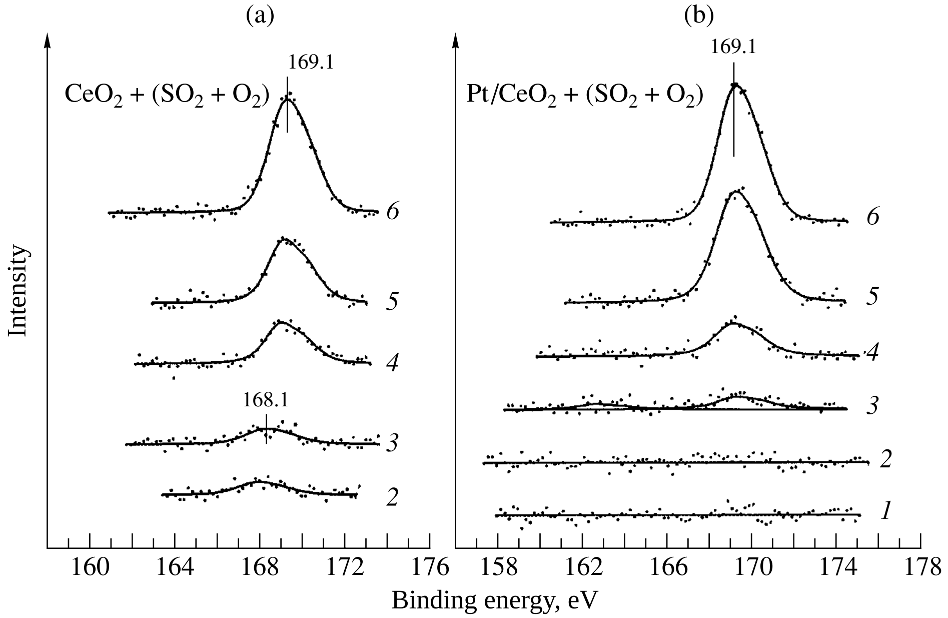

Fig. 4. XPS S2*p* spectra of (a) CeO_2 and (b) Pt/CeO_2 (*1*) before and after the reaction with a mixture of SO_2 and O_2 at $P_{SO_2} = P_{O_2} = 1.5 \times 10^2$ Pa and *T*, K: (*2*) 300, (*3*) 373, (*4*) 473, (*5*) 573, and (*6*) 673.

mon practice to denote the Ce3*d* spectra components (Ce(IV)) by the symbols v, v'', and v''' ($d_{5/2}$) or u, u'', and u''' ($d_{3/2}$); the corresponding binding energies are equal to 882.4, 889.0, and 898.3 or 900.8, 907.4, and 916.7 eV, respectively [21]. Fujimori [27] considered in detail the physical processes responsible for the appearance of these lines in the Ce3*d* spectrum. The deconvolution of lines presented in Fig. 5 suggests that the initial samples contained small amounts (~10–15%) of the reduced Ce(III) state, which corresponds to the Ce3*d* lines denoted by the symbols v' and u' with binding energies of 885.6 and 904.0 eV, respectively [21]. The other two lines intrinsic to the Ce(III) sate, v_0 and u_0 with binding energies of 880.6 and 898.9 eV, respectively, exhibited very low intensities with respect to the main doublet v'/u' [21]; therefore, they were not taken into account in the deconvolution. The spectra in Fig. 5a indicate that the reactions of CeO_2 with SO_2 and, to an even greater extent, with a mixture of SO_2 and oxygen resulted in the partial reduction of Ce(IV) to Ce(III), as evidenced by an increase in the intensities of v' and u' lines with the simultaneous weakening of lines due to Ce(IV). The reduction of cerium as a constituent of the model Pt/CeO_2 catalyst occurred more efficiently (Fig. 5b).

Figure 6a demonstrates quantitative data on the formation of sulfate and Ce(III) ions on the surface of CeO_2 in the reaction with SO_2-containing mixtures of different composition depending on reaction temperature. The S/Ce atomic ratio, which was determined from the intensity of the S2*p* signal with E_b ~169.2 eV and the total line intensity of the Ce3*d* spectrum after correcting for the corresponding atomic sensitivity factors [28], was taken as a measure of the amount of sulfate. The ratio of the total intensity of u' and v' lines to the total intensity of the Ce3*d* spectrum was used to characterize the fraction of Ce(III) ions. A comparison between diagrams in Figs. 6a and 6b allowed us to conclude that two processes occurred simultaneously: sulfate formation and CeO_2 reduction. The higher the yield of sulfate, the greater the fraction of reduced cerium.

The diagram in Fig. 6a also indicates that the capacity for CeO_2 sulfation decreased in the following order:

$$\begin{aligned} &CeO_2\text{: } (SO_2 + O_2 + H_2O) \\ &> (SO_2 + O_2) > SO_2 > (SO_2 + H_2O). \end{aligned} \tag{2}$$

This order is different from order (1) for Al_2O_3. The addition of oxygen to SO_2 is favorable for both sulfate formation and cerium dioxide reduction. The effect of water vapor is ambiguous. In a mixture with SO_2, water considerably decreased the tendency of CeO_2 to sulfation, although this decrease was not so high as in the case with Al_2O_3. In contrast, the addition of water to a mixture of SO_2 and oxygen increased both the formation of sulfate and the tendency of CeO_2 to reduction. The yield of sulfates and the fraction of reduced cerium increased with reaction temperature regardless of SO_2-containing reaction atmosphere.

DISCUSSION

An analysis of the S2*p* spectra measured after the interaction of Al_2O_3 and CeO_2 films and the oxide films containing sputtered platinum with SO_2 and a mixture of SO_2 + H_2O demonstrated that at moderate tempera-

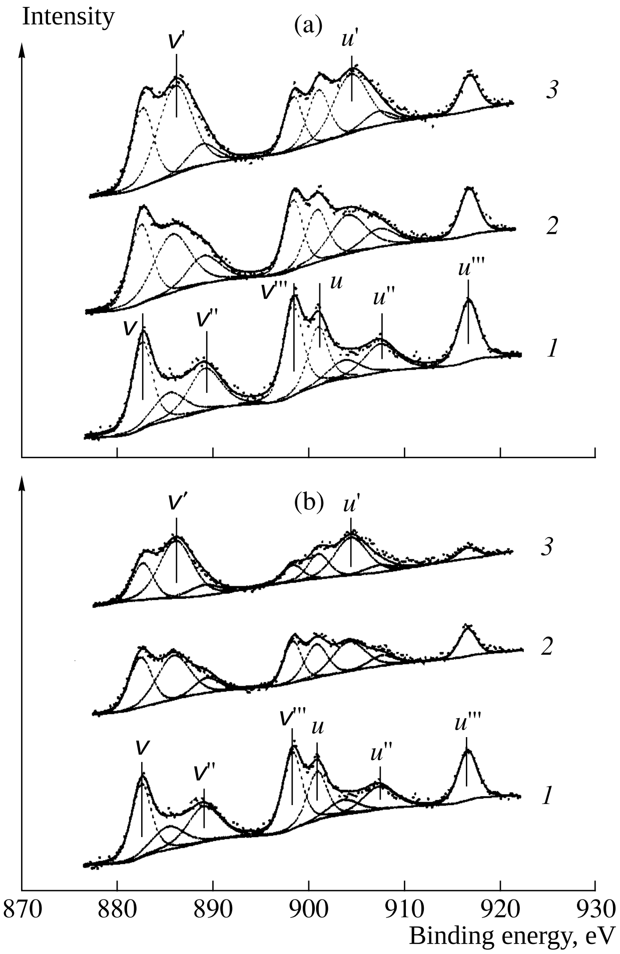

Fig. 5. XPS Ce3*d* spectra of (a) CeO_2 and (b) Pt/CeO_2 (*1*) before and after the reaction with (*2*) SO_2 or (*3*) a mixture of SO_2 and O_2 at $P_{SO_2} = P_{O_2} = 1.5 \times 10^2$ Pa and $T = 673$ K: *v*, *v*'', and *v*''' ($d_{5/2}$) and *u*, *u*'', and *u*''' ($d_{3/2}$) are Ce3*d* spectrum components responsible for Ce(IV).

tures (≤473 K) aluminum and/or cerium sulfates were formed. This result is consistent with data reported in many publications in which the formation of sulfites was found using IR spectroscopy, in particular, for Al_2O_3 [2–8] and CeO_2 [9, 13]. It was assumed that sulfite ions were formed upon the adsorption of SO_2 molecules on Lewis basic sites; surface O^{2-} ions can act as these sites [4]. The fact that the yield of sulfites in the reactions of oxides with SO_2 increased with oxide basicity [3, 9] is an additional argument in favor of this mechanism. It is believed that, on the surface of aluminum oxide, SO_2 is coordinated to the oxygen ion through the sulfur atom with the formation of structure **A** [10]. Next, this structure can be rearranged to structure **B** [5]:

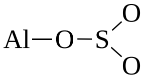

A

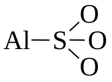

B

At the same time, the dramatic inhibition of the formation of aluminum and cerium sulfites on the addition of oxygen to the reaction mixture (cf. data in Figs. 1a and 2a, 3a and 4a) does not allow us to exclude the possibility of SO_2 adsorption at acid sites (Al^{3+}) through one of the oxygen atoms. Indeed, oxygen molecules can be adsorbed at Al^{3+} sites to render them inaccessible to SO_2 molecules. Such an effect of oxygen on the adsorption of SO_2 at basic sites is highly improbable.

The process of sulfate formation from SO_2 requires a change in the oxidation state of sulfur. Therefore, it occurs more readily in the presence of oxygen: it began at lower temperatures and resulted in greater amounts of sulfates (cf. data in Figs. 1a and 2a, 3a and 4a). This result was also supported by published data: the treatment of sulfites, which were prepared in the reaction of alumina with SO_2, with oxygen or the interaction of Al_2O_3 with a mixture of SO_2 and O_2 at $T \sim 673–973$ K resulted in the formation of sulfates [2, 3, 6, 8, 11, 12, 16]. With the use of IR spectroscopy, it was found [11, 29] that the sulfate ion forms structure **C** on the surface of alumina. Structures **D** and **E** were proposed [17, 30] for surface aluminum sulfate.

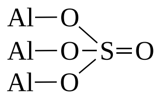

C

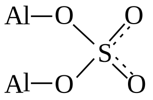

D

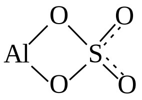

E

In the case when a metal oxide exhibits oxidizing properties, the interaction of the oxide with SO_2 to form sulfates can also occur without the participation of oxygen. It was reported that the reactions of SO_2 with manganese oxides (Mn_2O_3 and MnO_2) [31] and a tin oxide (SnO_2) [20] gave $MnSO_4$ and $SnSO_4$ sulfates, respectively. However, in none of the cases was the decrease in the oxidation state of the metal confirmed. For CeO_2, sulfates can also be obtained in the absence of oxygen. According to IR-spectroscopic data, the heating of CeO_2 with sulfite, which was prepared by the interaction with SO_2, in a vacuum resulted in sulfate formation [7]. As found using UV reflectance spectroscopy, the process of sulfate formation was accompanied by cerium reduction to Ce(III) [13]. At the same time, sulfates on the surface of CeO_2 were detected by XPS and X-ray adsorption near-edge structure (XANES) spectroscopy even after SO_2 adsorption at room temperature [14]. In this case, no changes in the charge state of cerium were detected by measuring the valence-band photoemission spectra. On this basis, Rodriguez *et al.* [14] considered that the disproportionation of SO_2 to Ce(IV) sulfate and SO took place. However, the results obtained in this work suggest that sulfate formation occurred simultaneously with the reduction of Ce(IV) to Ce(III); this allowed us to assume the occurrence of the following reaction:

$$6CeO_2 + 3SO_2 \longrightarrow Ce_2(SO_4)_3 + 2Ce_2O_3. \qquad \text{(I)}$$

The formation of Ce(III) sulfate is an activated process, which requires heating to $T \geq 573$ K. In the presence of

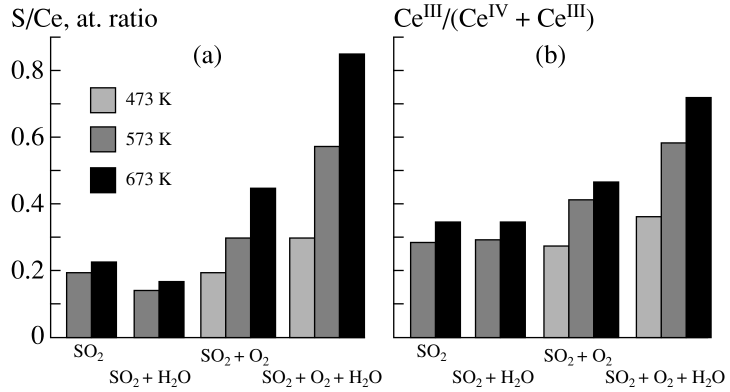

Fig. 6. (a) Changes in the S/Ce atomic ratio determined from sulfate S2*p* and Ce3*d* line intensities and (b) the fraction of Ce(III) as a constituent of the CeO_2 surface depending on the composition of the reaction gas mixture and on the temperature.

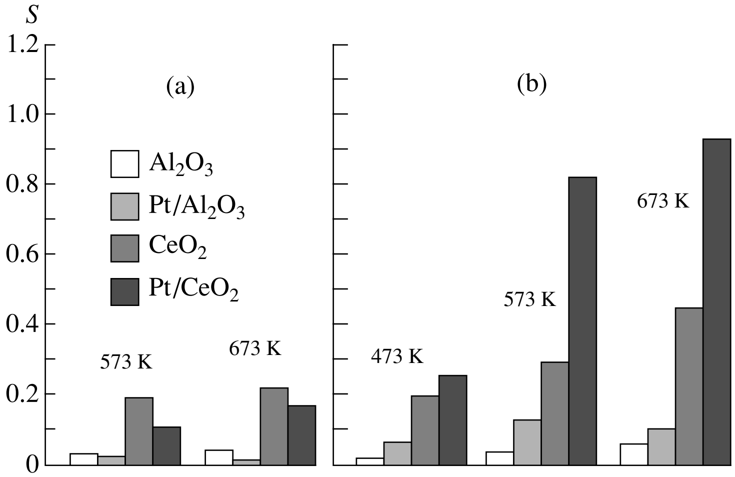

Fig. 7. Changes in the yield of sulfate (*S* is the S2*p* (SO_4^{2-})/Ce3*d* or S2*p* (SO_4^{2-})/Al2*p* atomic ratio) depending on the composition of the model catalytic system, the presence of oxygen in the reaction mixture ((a) SO_2 and (b) $SO_2 + O_2$), and the temperature.

oxygen, the process occurred at a lower temperature and with a higher yield. It is likely that in this case the following reaction can take place:

$$2CeO_2 + 3SO_2 + O_2 \longrightarrow Ce_2(SO_4)_3. \qquad \text{(II)}$$

Taking into account the redox character of sulfate formation, the detection of sulfates seems unexpected in the case of the reaction of Al_2O_3 with SO_2 in the absence of oxygen (Fig. 1a). In other studies performed with the use of IR spectroscopy, the formation of only sulfites was observed under the specified conditions [2–8]. On the other hand, in many studies performed using XPS and XANES techniques, sulfates were detected even after low-temperature SO_2 adsorption on the surfaces of oxides such as ZnO [32] and MgO [33], in which metal ions are also not prone to changes in the oxidation state. As in this work, the detection of the $S2p_{3/2}$ line in the region ~168–169.5 eV in the XPS spectrum was related to sulfate formation. It is believed that an adsorption state with structure **D** or **E** was formed in this case. The disproportionation of SO_2 also cannot be excluded; evidently, additional experiments are required to refine the structure of sulfates in the case of aluminum oxide, and these experiments may be performed using IR spectroscopy.

The formation of aluminum and cerium sulfites and sulfates was also detected in the reactions of SO_2 with the model catalytic systems Pt/Al_2O_3 and Pt/CeO_2. The presence of platinum manifested itself in the simultaneous sulfide formation on the Pt surface. The adsorption of SO_2 on the surface of Pt single crystals was studied [34, 35]; these studies demonstrated that adsorbed SO_2 molecules dissociated into atoms at $T \sim 300$ K. The reactive atoms of oxygen adsorbed on platinum were removed because of reactions with background gases (CO and hydrocarbons) to leave sulfur atoms on the surface of platinum particles. The sulfur atoms reacted with platinum to form a surface sulfide. It is likely that the presence of oxygen in the reaction mixture suppressed sulfide formation because of sulfide oxidation.

Figure 7 shows two diagrams that compare the yields of sulfates depending on the compositions of the test films and the reaction gas mixtures and on the temperature. As follows from the diagram in Fig. 7a, the yield of sulfates formed in the reaction of SO_2 without oxygen decreased on going from the pure oxide to the oxide with supported platinum. When Pt/Al_2O_3 and Pt/CeO_2 reacted with a mixture of SO_2 and O_2, sulfates became predominant products, especially at elevated temperatures (Figs. 2b, 4b). It can be seen (Fig. 7b) that the sputtering of platinum onto both oxides significantly increased the yield of sulfates. This was likely due to the more effective activation of oxygen on Pt particles, as compared with oxide surfaces.

In conclusion, note that the formation of sulfates occurred more effectively on CeO_2, as compared with Al_2O_3, regardless of the composition of the SO_2-containing mixture, the reaction temperature, and the presence of platinum on the oxide surface.

REFERENCES

1. Truex, T.J., *SAE Paper*, 1999, Paper no. 1999-01-1543.
2. Chang, C.C., *J. Catal.*, 1978, vol. 53, p. 374.
3. Babaeva, M.A., Tsyganenko, A.A., and Filimonov, V.N., *Kinet. Katal*., 1984, vol. 25, p. 787.
4. Karge, H.G. and Dalla Lana, I.G., *J. Phys. Chem.*, 1984, vol. 88, p. 1538.
5. Datta, A., Cavell, R.G., Tower, R.W., and George, Z.M., *J. Phys. Chem.*, 1985, vol. 89, p. 443.
6. Nam, S.W. and Gavalas, G.R., *Appl. Catal.*, 1989, vol. 55, p. 193.
7. Waqif, M., Saad, A.M., Bensitel, M., Bachelier, J., Saur, O., and Lavalley, J.C., *J. Chem. Soc., Faraday Trans.*, 1992, vol. 88, p. 2931.
8. Mitchell, M.B., Sheinker, V.N., and White, M.G., *J. Phys. Chem.*, 1996, vol. 100, p. 7550.
9. Ziolek, M., Kujawa, J., Saur, O., Aboulayt, A., and Lavalley, J.C., *J. Mol. Catal., A: Chem.*, 1996, vol. 112, p. 125.
10. Saad, A.B.M., Saur, O., Wang, Y., Tripp, C.P., Morrow, B.A., and Lavalley, J.C., *J. Phys. Chem.*, 1995, vol. 99, p. 4620.
11. Saur, O., Bensitel, M., Saad, A.B.M., Lavalley, J.C., Tripp, C.P., and Morrow, B.A., *J. Catal.*, 1986, vol. 90, p. 104.
12. Waqif, M., Saur, O., Lavalley, J.C., Perathoner, S., and Centi, G., *J. Phys. Chem.*, 1991, vol. 95, p. 4051.
13. Waqif, M., Bazin, P., Saur, O., Lavalley, J.C., Blanchard, G., and Touret, O., *Appl. Catal., B,* 1997, vol. 11, p. 193.
14. Rodriguez, J.A., Jirsak, T., Freitag, A., Hanson, J.C., Larese, J.Z., and Chaturvedi, S., *Catal. Lett.*, 1999, vol. 62, p. 113.
15. Overbury, S.H., Mullins, D.R., Huntley, D.R., and Kundakovic, Lj., *J. Phys. Chem.*, 1999, vol. 103, p. 11308.
16. Uy, D., Dubkov, A., Graham, G.W., and Weber, W.H., *Catal. Lett.*, 2000, vol. 68, p. 25.
17. Dosumov, K., Umbetkaliev, A.K., and Popova, N.M., *Zh. Prikl. Khim.*, 1994, vol. 67, p. 1961.
18. Loof, P., Kasemo, B., Bjornkvist, L., Andersson, S., and Frestad, A., *Catalytic and Automotive Pollution Control II*, Crucq, A., Ed., Amsterdam: Elsevier, 1991, p. 253.
19. Bazin, P., Saur, O., Lavalley, J.C., Blanchard, G., Visciglio, V., and Touret, O., *Appl. Catal., B*, 1997, vol. 13, p. 265.
20. Gergely, B., Guimon, C., Gervasini, A., and Auroux, A., *Surf. Interface Anal.*, 2000, vol. 30, p. 61.
21. Romeo, M., Bak, K., El Fallah, J., Le Normand, F., and Hilaire, L., *Surf. Interface Anal.*, 1993, vol. 20, p. 508.
22. Kalinkin, A.V. and Pashis, A.V., *React. Kinet. Catal. Lett.*, 1992, vol. 46, pp. 33, 39.
23. Kalinkin, A.V., Savchenko, V.I., and Pashis, A.V., *Catal. Lett.*, 1999, vol. 59, p. 115.
24. *NIST X-Ray Photoelectron Spectroscopy Database*, 1997.
25. Visser, J.P.R., Groot, C.K., van Oers, E.M., de Beer, V.H.J., and Prins, R., *Bull. Soc. Chim. Belg.*, 1984, vol. 93, p. 813.
26. Wang, T., Vazques, A., Kato, A., and Schmidt, L.D., *J. Catal.*, 1982, vol. 78, p. 306.
27. Fujimori, A., *J. Magn. Magn. Mater.*, 1985, vols. 47–48, p. 243.
28. *Practical Surface Analysis by Auger and X-Ray Photoelectron Spectroscopy*, Briggs D. and Seach M.P., Eds., New York: Wiley, 1983.
29. Dunn, J.P., Jehng, J.M., Kim, D.S., Briand, L.E., Stenger, H.G., and Wachs, I.E., *J. Phys. Chem. B*, 1998, vol. 102, p. 6212.
30. Khadzhivanov, K. and Davydov, A.A., *Kinet. Katal.*, 1988, vol. 29, p. 398.
31. Kijlstra, W.S., Biervliet, M., Poels, E.K., and Bliek, A., *Appl. Catal., B*, 1998, vol. 16, p. 327.
32. Rodriguez, J.A., Jirsak, T., Chaturvedi, S., and Kuhn, M., *Surf. Sci.*, 1999, vol. 442, p. 400.
33. Rodriguez, J.A., Pérez, M., Jirsak, T., González, L., and Maiti, A., *Surf. Sci.*, 2001, vol. 477, p. 279.
34. Sun, Y.-M., Sloan, D., Alberas, D.J., Kovar, M., Sun, Z.-J., and White, J.M., *Surf. Sci.*, 1994, vol. 319, p. 34.
35. Zebisch, P., Stichler, M., Trischberger, P., Weinelt, M., and Steinruck, H.-P., *Surf. Sci.*, 1997, vol. 371, p. 235.